Baghdad Science Journal

Volume 23 | Issue 2 Article 5

2-23-2026

Synthesis, Spectroscopic Characterization, and Photostability Studies of a New Ligand Derivative of 4-Bromobenzaldehyde and its Metal Complexes

Enass J. Waheed
Department of Chemistry, College of Education for Pure Sciences, Ibn -Al-Haitham, University of Baghdad, Baghdad, Iraq, enass.j.w@ihcoedu.uobaghdad.edu.iq

Ali Mudher Abdulkareem
Department of Chemistry, College of Education for Pure Sciences, Ibn -Al-Haitham, University of Baghdad, Baghdad, Iraq, ali.m.ak@ihcoedu.uobaghdad.edu.iq

Ibtisam Khalifa Jassim
Department of Chemistry, College of Education for Pure Sciences, Ibn -Al-Haitham, University of Baghdad, Baghdad, Iraq, Ibtisam.kh@ihcoedu.uobaghdad.edu.iq

How to Cite this Article

Waheed, Enass J.; Abdulkareem, Ali Mudher; and Jassim, Ibtisam Khalifa (2026) "Synthesis, Spectroscopic Characterization, and Photostability Studies of a New Ligand Derivative of 4-Bromobenzaldehyde and its Metal Complexes," *Baghdad Science Journal*: Vol. 23: Iss. 2, Article 5.
DOI: https://doi.org/10.21123/2411-7986.5197

BAGHDAD SCIENCE JOURNAL 2026;23(2):462–477

RESEARCH ARTICLE

Synthesis, Spectroscopic Characterization, and Photostability Studies of a New Ligand Derivative of 4-Bromobenzaldehyde and its Metal Complexes

Enass J. Waheed *, **Ali Mudher Abdulkareem**, **Ibtisam Khalifa Jassim**

Department of Chemistry, College of Education for Pure Sciences, Ibn -Al-Haitham, University of Baghdad, Baghdad, Iraq

ABSTRACT

The new Schiff base ligand (L_B) was synthesized by reacting precursor (P) with 4-bromobenzaldehyde. This ligand formed three new complexes: $[Pd(L_B)(H_2O)_2]Cl_2$ (square planar) and $[M(L_B)(H_2O)_2Cl_2]\cdot mCl_2$ (octahedral), where m=0 for Co^{+2} and 1 for Pt^{+4}, upon reaction with the respective metal ions. Characterization of the ligand (L_B) and its metal complexes involved various techniques including ^{1}H- and ^{13}C-NMR, FT-IR, UV-Vis spectroscopy, magnetic susceptibility measurements, CHNS analysis, and molar conductivity. The photo-stabilization of polymers aims to mitigate or delay photochemical degradation during irradiation of plastic materials like polyvinyl chloride (PVC) in tetrahydrofuran (THF). Prepared compounds (ligand L_B and its metal complexes) were incorporated into PVC at 0.5% w/w concentration. Under irradiation with light at $\lambda = 380–250$ nm and intensity of 7.75×10^{-9} ein $dm^{-3}\,s^{-1}$ at 25°C, the photo-stabilization efficacy of these additives was evaluated by monitoring changes in carbonyl, polyene, and hydroxyl indices over time, using weight loss as a measure. Observations showed that I_{CO}, I_{OH}, and I_{PO} index values increased with irradiation time, varying depending on the additive type. Surface morphology of the films was also studied over time. This application holds significance for environmental conservation by addressing concerns related to plastic consumption reduction.

Keywords: 4-bromobenzaldehyde, Metal complexes, Photodegradation, Photo-stabilization, Polyvinyl chloride

Introduction

Polymers play a crucial and essential role in various fields and human activities. The choice of polymer—whether raw, nanocomposite, or polymer mixtures—depends on the specific need. Modifying the properties of polymers is possible through alterations of functional and structural groups[1] or by integrating reinforcing fillers. Numerous studies have addressed these modifications. Various classes of polymeric composites can be developed based on the selected reinforcement, such as nanocomposites, fiber-filled composites, and microcomposites.[2] Polyvinyl chloride (PVC) is one of the most important thermoplastic vinyls, especially considering its application range and production volume. It is extensively used in many fields, from building materials to healthcare products.[3] Its limited applications in supporting catalysts and organic synthesis, as mentioned in previous literature, have sparked current interest and development. Schiff's base is an organic compound containing the azomethine group (C=N-). It was first prepared in 1864 by the scientist Schiff through the condensation of a carbonyl group (CO) with a primary amine (R–NH_2) or an aromatic amine (Ar–NH_2). The carbonyl group of the ketone/aldehyde reacts with the carbon, forming an intermediate compound (carbinol-amine), which then loses an H_2O molecule to form an N-substituted imine. This final compound, representing a chelated base, has various names, including imines. When derived from a ketone, they are called ketimines, and when derived from an

Received 21 May 2024; revised 20 September 2024; accepted 22 September 2024.
Available online 23 February 2026

* Corresponding author.
E-mail addresses: enass.j.w@ihcoedu.uobaghdad.edu.iq (E. J. Waheed), ali.m.ak@ihcoedu.uobaghdad.edu.iq (A. M. Abdulkareem), Ibtisam.kh@ihcoedu.uobaghdad.edu.iq (I. K. Jassim).

https://doi.org/10.21123/2411-7986.5197

aldehyde, they are called aldimines.[4,5] Heterocyclic compounds represent an important class of biologically active molecules. Furthermore, many heterocyclic compounds and bioactive compounds contain a five-membered heterocyclic ring of nitrogen, sulfur, and oxygen.[6] Heterocyclic compounds are an important class of biologically active molecules. Many bioactive compounds and heterocyclic compounds contain a five-membered heterocyclic ring with nitrogen, sulfur, and oxygen. cefixime belongs to the third-generation cephalosporin antibiotics. It is highly effective against many types of bacteria, and it fights diseases by stopping the growth of the bacteria that cause them. Cefixime[7] is effective in treating infections such as laryngitis, pneumonia, otitis media, tonsillitis, gonorrhea, urinary tract infections and pharyngitis.[8,9] 4-Bromobenzaldehyde is an intermediate substance used in the preparation of pharmaceutical preparations, organic compounds, and agricultural chemicals. It acts as a precursor and reacts with sulfamethoxazole to prepare a Schiff base, which is used in the photo-stability of polyvinyl chloride. It is also used in cross-coupling[10] studies with $C_2H_3BF_3K$ and in the Pd-catalyzed mono- and diarylation of 3,4-ethylenedioxythiophene (EDOT).[11] The interactions between metal ions and antibiotics are significant because they influence the preparation of metal antibiotics through interactions between absorbed drugs and metal ions.[7] Complexes containing Schiff base ligands have garnered significant attention due to their numerous applications in medical, food, analytical, dyes, and chemical catalysis fields, largely due to their simple preparation[12] and chemical catalysis fields due to the simplicity of their preparation'.[13] In this study, a ligand (L_B) was prepared by reacting 4-bromobenzaldehyde with a precursor (p) and then reacting it with selected metal ions (M = Pt^{+4}, Pd^{+2}, Co^{+2}) to produce metal complexes. Finally, the photostability of the prepared compounds was studied.

Materials and methods

Chemicals were used as they are of high purity without any purification and prepared by certified companies (BDH, Fluka or Merck). To prepare PVC films, a German 1000mm/40inch Vogel digital caliper is adopted. Based on a Meiji Techno microscope (Meiji Techno, Tokyo, Japan), (magnification × 460), the morphological images of polyvinyl chloride films were recorded. Measurement of electronic transfers of compounds prepared at laboratory temperature and with a quartz cell (1cm) was carried out using a device UV-M90 Double Beam Spectrophotometer. Analysis of microelements (CHNS) was performed using a device Euro EA CHNSO Elemental Analyzer. Infrared spectroscopy was performed for the prepared compounds within the range (4000–400) cm^{-1} with potassium bromide tablets using a device Shimadzu FTIR-8400S Spectrometer. Electrical conductivity measurement was performed at concentration (10^{-3} M) and laboratory temperature with DMSO solvent by a Philips pw - Digital Meter Conductance. The atomic absorption measurement of complexes was carried out using a device Shimadzu AA-7000 Shimadzu. An examination of the magnetic susceptibility of metal complexes was carried out at temperature 25 °C using a device the Sherwood Scientific's Magnetic Susceptibility Balances. ^{1}H-, ^{13}C-NMR spectroscopic measurements of the prepared ligand was performed using a device Bruker AVANCE NEO 400 MHz spectrophotometer with DMSO. Determination of chlorine content in the prepared compounds was carried out using 686-Titro processor – 665 Dosimat. Metrohm. Swiss. By a Stuart SMP10 m.p Apparatus, the m.p of the ligand (L_B) and its complexes was measured.

Synthesis of New Schiff base ligand (L_B)

Synthesis ligand (L_B) in two steps

A-Synthesis of precursor (P)[14]

Using a 100mL round flask, (0.47g, 1mmol) of cefixime was dissolved in (1mL) of absolute ethanol containing dissolved HCl, where saturated absolute ethanol was prepared. With HCl gas, by adding an amount of concentrated sulfuric acid to a flask containing an amount of sodium chloride (NaCl), and we collect the liberated gas in a flask containing ethanol, which is formed (ethanol saturated with HCl gas) and the mixture is left to stir continuously. With reflux for 3 hrs, the course of the reaction was followed by TLC. After that, the mixture was cooled to obtain ester crystals, and they were recrystallized using hot methanol and diethyl ether. The percentage of the product after drying the precipitate was 85% and its melting points were 109–111 °C.

B-Synthesis of new-Schiff base-Ligand (L_B)

The (L_B) was prepared by adding a solution of the substance obtained in the first step (P) (0.51g, 1mmol) in 10 mL of EtOH to a solution of (4-bromobenzaldehyde) (0.14g, 1mmol in 10 mL of ethanol with the addition of (3-4) drops of glacial acetic acid. After stirring for one hour, the mixture was placed under reflux for 3 hours, and then the course of the reaction was followed by TLC. After that, the mixture was filtered to obtain the desired precipitate (orange), and the precipitate was

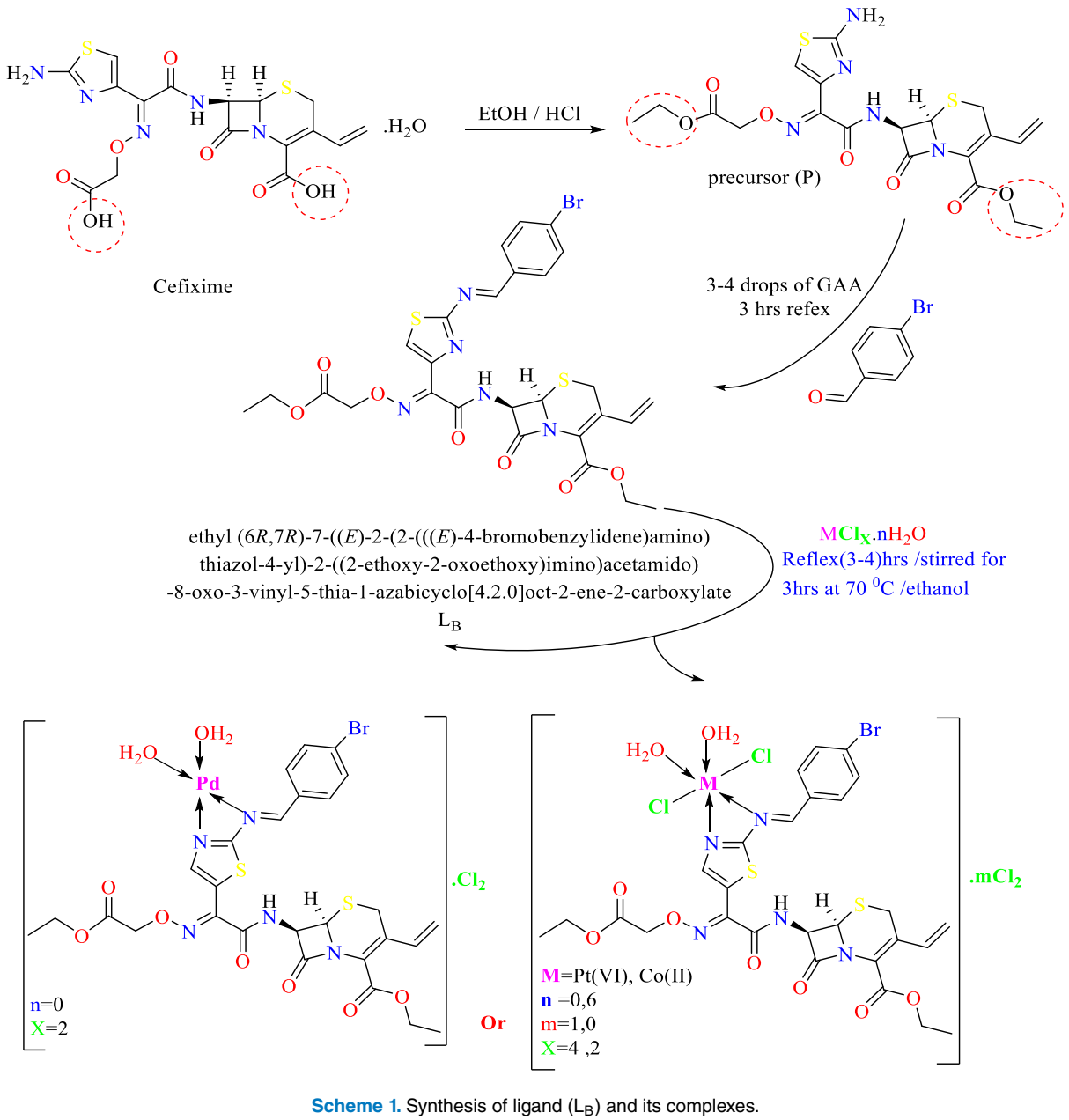

Scheme 1. Synthesis of ligand (L_B) and its complexes.

recrystallized using hot methanol and diethyl ether. The product was then left to dry at lab temperature and was weighed to calculate the percentage of the product, which was 79%. And the melting point is 135–137 ˚C, Scheme 1.

Synthesis of the complexes[15]

The cobalt complex was prepared with a molar ratio of (1:1) (M:L) using a 100mL round flask by adding (0.17gm). (1mmol) of cobalt chloride ($CoCl_2.6H_2O$) dissolved in (10mL) ethanol to the ligand solution (L_B) resulting from dissolving (0.24gm, 1mmol) in (10mL) ethanol and leave the mixture at a temperature of 70 ˚C with continuous stirring and reflux for 3 hours. Filter the solution to obtain the green precipitate. Then washing with distilled water and diethyl ether until recrystallization with absolute methanol. The percentage of the product, which was 65%, and the melting point (195-197) ˚C were calculated. The Pt^{+4}, Pd^{+2} and Co^{+2} complexes were synthase by the same method mentioned, Scheme 1.

Films preparation technique of (PVC)[16]

The (PVC) was dissolved in a w/v 0.5% solution of solvent (THF). After preparation was completed, the solutions were poured into a glass frame. With the

Table 1. Physical properties of (LB) and complexes.

Com.	Color	M.wt	Melting point	Elemental analysis Found (Calc.) (%) M	C	H	N	S	Cl
(L_B) $C_{27}H_{26}BrN_5O_7S_2$	Orange	676.56	135–137 ^{0}C	-	47.87 (47.93)	3.50 (3.87)	10.72 (10.35)	9.35 (9.48)	-
$[Pt(L_B)(H_2O)_2Cl_2].2Cl_2$	Yellow	1049.47	260–262 ^{0}C	18.63 (18.59)	30.44 (30.90)	2.56 (2.88)	6.83 (6.67)	6.47 (6.11)	13.60 (13.51)
$[Pd(L_B)(H_2O)_2].Cl_2$	Dark orange	889.91	215–217 ^{0}C	11.77 (11.96)	36.67 (36.44)	3.58 (3.40)	7.66 (7.87)	7.34 (7.21)	7.88 (7.97)
$Co(L_B)(H_2O)_2Cl_2]$	Green	842.42	195–197 ^{0}C	7.22 (7.00)	38.62 (38.50)	3.37 (3.59)	8.56 (8.31)	7.54 (7.61)	8.38 (8.42)

creation of small sinks with 4 ml capacity, based on attaching laboratory glass slides to a piece of regular glass to obtain this frame. Upon reaching 18 hours, the solvent began to evaporate causing the polymer sheets to appear. The thickness of the films was about 40 micrometers, and they were pasted on sheets of paper with holes measuring 2.5×2.5 cm^2.

Results and discussion

Some properties of coordination compounds were studied, including the nature of the colored solid and thermal stability. A great match was also found between the theoretical data and the practical results of (CHNS) of synthases compounds, as in Table 1.

FT-IR spectra

In Table 2, the ligand (L_B) was identified by studying its infrared spectrum shown in Fig. 1, where strong band at (3279) cm^{-1} cm was observed, is attributed to the frequency $\upsilon(N–H)_{str}$. As for the two sharp, strong bands at wave numbers 1739 cm^{-1} and 1693 cm^{-1}, they are attributed to the stretching frequency bands of the carbonyl group $\upsilon(C=O)_{ester}$ and $\upsilon(C=O)_{amid}$e respectively, with the appearance of other stretching frequency bands at (1589)cm^{-1}, (1516)cm^{-1} and (1226,1172)cm^{-1} belong to the aggregates $\upsilon(C=N)_{five\ ring}$, $\upsilon(N\text{-}H)_{bend}$, $\upsilon(C\text{-}O\text{-}C)_{ester}$ respectively and finally a band appears at the wave number 1635 cm^{-1} is due to $\upsilon(CH=N)_{imine}$ for the ligand (L_B). [17,18]

Infrared measurements were carried out for the metal complexes and the prepared ligand (L_B), and the difference occurring between them was studied. It was observed that some bands shifted and new bands appeared while other bands remained stable. The infrared spectra of the metal complexes of the ligand showed (L_B) represented by Fig. 1 is absorption bands within the range 3417-3232 cm^{-1}, 1743-1735 cm^{-1} and 1697-1681 cm^{-1} attributed to $\upsilon(N–H)_{str}$., $\upsilon(C=O)_{ester}$ and $\upsilon(C=O)_{amide}$ respectively, which did not participate in the coordination of the prepared complexes, while the coordination of the ligand (L_B) with the metal ions was revealed through absorption bands of the order of 1647-1635 and 1608-1597 cm^{-1}, which are attributed to the groups of $\upsilon(C=N)_{imine}$ and $\upsilon(C=N)_{five\ ring}$ respectively, which were shifted towards different frequencies compared to their

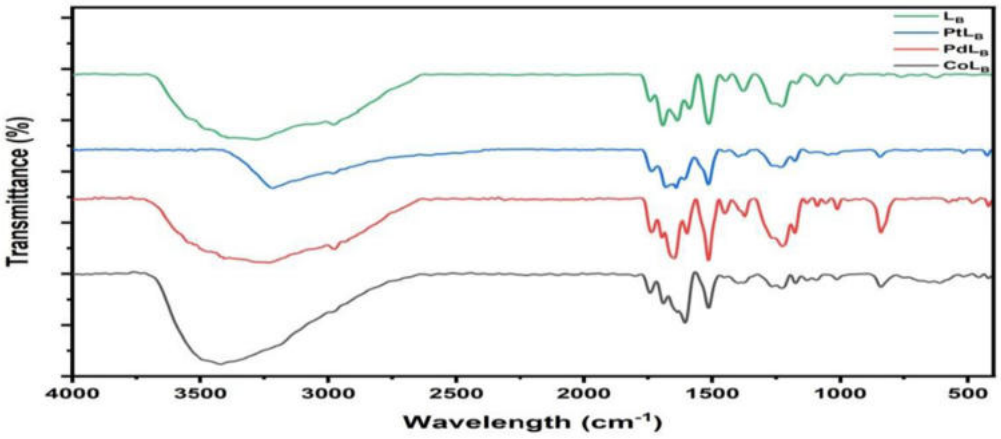

Fig. 1. FTIR spectrum of LB and its complexes.

Table 2. FTIR data of LB with complexes.

Com.	υ(N - H) str. υ(N - H) bend	υC = O) υ(COC) ester	υ (C=N) five ring	υ (C=O) amide	υ (C=N) imine	ρ (H2O)	υ(M-N) υ (M-N)
(L_B)	3279 1516	1739 1226 1172	1589	1693	1635	-	-
$[Pt(L_B)(H_2O)_2Cl_2].2Cl_2$	3213 1516	1735 1234 1176	1608	1681	1639	840	516 424
$[Pd(L_B)(H_2O)_2].Cl_2$	3232 1516	1735 1226 1176	1597	1697	1647	837	482 420
$Co(L_B)(H_2O)_2Cl_2]$	3417 1516	1743 1230 1172	1604	1689	1635	839	455 420

Table 3. Proton NMR data for ligand LB with DMSO-d^6

Ligand	Protons Type	Protons number	δ (ppm)
	6H, proton $2CH_3$ group	H11	1.03–1.71
	4H, proton $2O\text{-}CH_2$ group	H10	3.41–3.47
	4H, proton $S\text{-}CH_2$ + $O^-CH_2C{=}O$ group	H4, H26	4.15–4.52
L_B	5H, proton C-H group	H6, H7, H12, H13	4.88–4.97
	4H, proton C-H aromatic group	H23, H24	6.77–7.94
	1H, proton NH group	——-	8.20
	1H, proton N=CH group	H21	8.58
	1H, proton C=CH-S group	H20	10.00

Table 4. Carbon NMR data for ligand LB with DMSO-d^6

Ligand	Carbons kind	Carbons number	δ (ppm)
	2C, CH_3	C11	19.00
	1C, $S\text{-}CH_2$	C4	26.65
	1C, N-CH	C7	56.49
	2C, $O\text{-}CH_2$	C10	60.83
	1C, S-C-N	C6	61.82
	1C, $NOCH_2$	C26	72.04
	1C, $=CH_2$	C13	115.31
	1C, N-C=	C2	117.32
	1C, S-CH=	C20	128.93
L_B	2C, CH aromatic	C23	129.83
	1C, =CH	C12	131.22
	2C, CH aromatic	C24	131.66
	1C, C aromatic	C22	135.27
	1C, C-Br	C25	136.79
	1C, =C	C3	139.85
	1C, =C	C19	147.27
	1C, C=N	C15	156.26
	1C, C=N	C21	160.50
	1C, NHCO	C14	163.17
	1C, NC=O	C8	164.85
	1C, OC=O	C9	165.78
	1C, OC=O	C27	168.39
	1C, N=C-N	C17	178.55

absorption band in the free ligand (L_B). What enhances this consistency is the appearance of weak absorption bands in the range 582-516 and 424-420 cm^{-1} attributed to the υ(M-N) and υ(M-N) bands in the complexes. What confirms the coordination of water with the central ion is the appearance of bands within the range 840-837 cm^{-1}, dating back to ρ(H_2O) in the spectra of metal complexes,[19,20] Table 2.

^{1}H-, ^{13}C-NMR spectra

The Proton NMR spectral data of ligand L_B is listed in Table 3, Fig. 2-A.

The Carbon NMR data of ligand L_B is listed in Table 4, Fig. 2-B.

Electronic spectra

The electronic transitions associated with the prepared compounds of the ligand L_B and its metal complexes were listed in both the Table 5, and Fig. 3, noting the differences occurring between them, which confirm the coordination.[21,22]

Photo stability

The photo stability of the (L_B) new Schiff base ligand and (Co^{+2}, Pd^{+2}, and Pt^{+4}) complexes was assessed by modifying them with polyvinyl chloride (PVC) sheets and dissolving them in tetrahydrofuran (THF) at a temperature of 25 °C. The 3450–3200 cm^{-1} band in the FTIR spectrum has a significant occurrence that reduces the intensity of the band. This occurrence is the reason for the synthesis of OH (I_{OH}), polyene (I_{PO}), and CO (I_{CO}), groups, show in Fig. 4. The indices I_{OH}, I_{CO}, and I_{PO} are shown in Figs. 5 to 7 respectively. These figures illustrate the time of increased susceptibility to radiation compared to PVC without any additives, resulting in an elevated exposure rate for I_{OH}, I_{CO}, and I_{PO}.

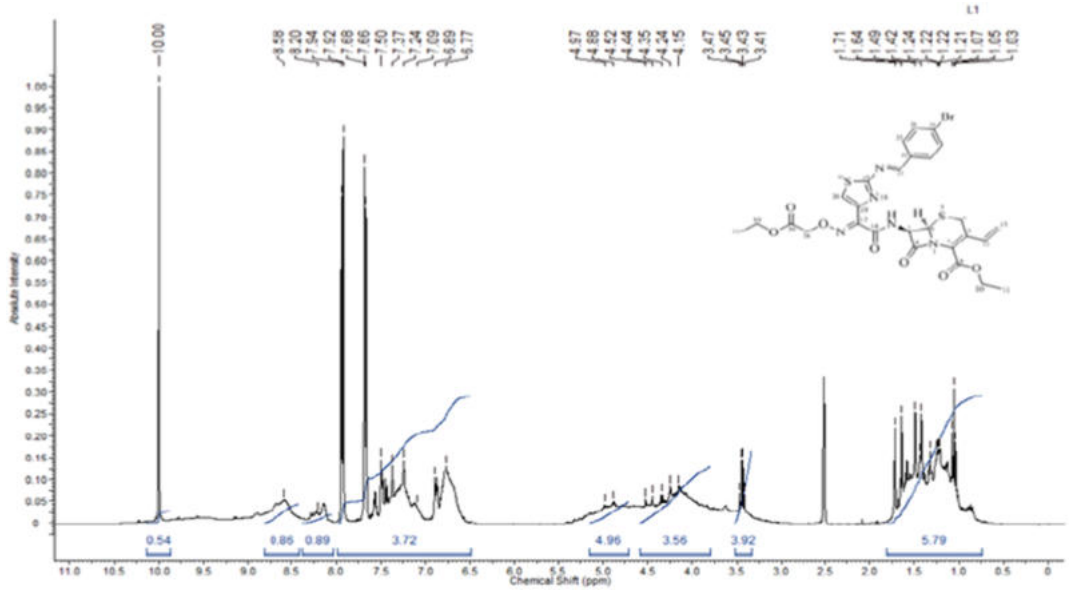

Fig. 2-A. ^{1}H-NMR spectrum of ligand L^{B}.

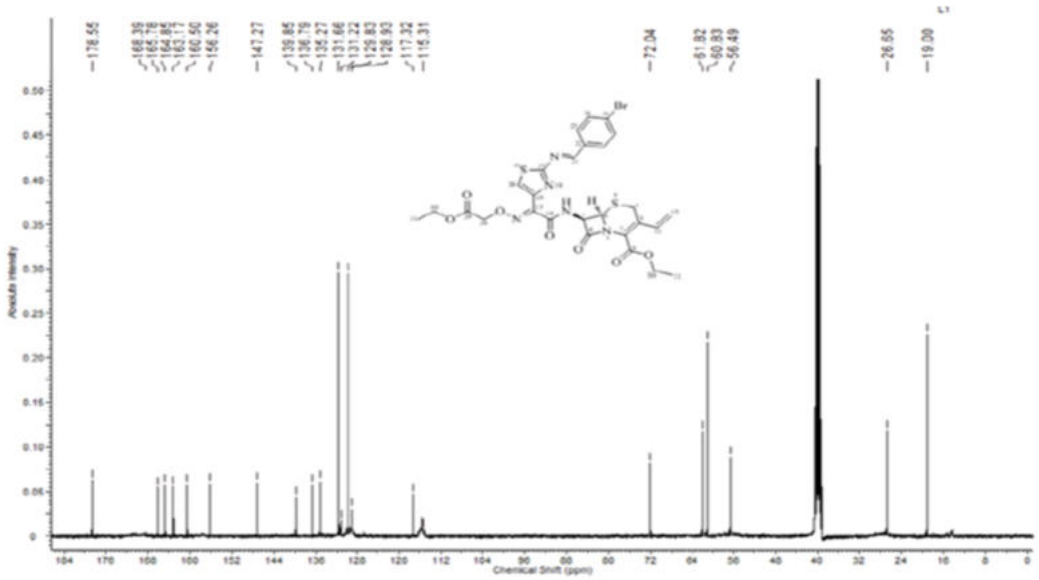

Fig. 2-B. ^{13}C-NMR spectrum of ligand L^{B}.

Figs. 5 to 7 demonstrate a notable increase in the exposure rate of (I_{OH}), (I_{CO}), and (I_{PO}) Indices when compared to PVC films that do not have a sensitive irradiation time. The addition of metal ions like Co^{+2} and Pd^{+4} suggests that Pt^{+4} is the most effective as an image stabilizer.

Effect photolysis on polyvinyl chloride films in terms of molecular weight

The relationship between the irradiation time and the retrograde rate (α), is shown in the graph of Fig. 8, the rapid decrease in $\overline{Mv}$ was caused by the collapse of a large chain far away in the PVC chain as in Fig. 9, which shows that the degradation of PVC is due to the decrease in PVC scale. That the film was exposed to radiation an additional 0.5% of the time was proven by the Mv versus exposure plot. S represents the actual population of chain scissors in Fig. 10, Eq. (1).

$\overline{Mv}$, 0 = Molecular weight viscosity represents at the experiment foremost.
$\overline{Mv}$,t = Molecular weight viscosity represents on average by the irradiation.

$$S = \overline{Mv}, 0/\overline{Mv}, t - 1 \quad (1)$$

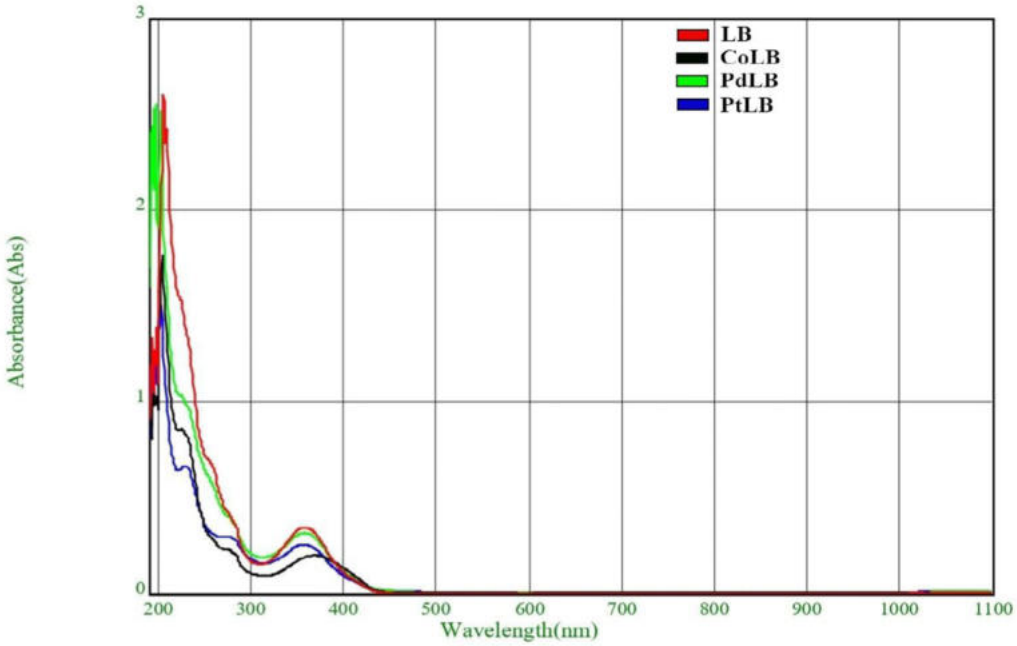

Fig. 3. Electronic spectrum of ligand LB and its complex.

Table 5. UV/Vis data of ligand LB with complexes.

Compound	Maximum absorption υmax(cm^{-1}) and (nm)	Band assignment	Molar Conductivity (Electrolyte nature)	μeff (B.M)	Suggested geometry
L_B	34482(290) 29325(341)	$\pi \rightarrow \pi^*$ n$\rightarrow \pi^*$	-	-	-
$[Pt(L_B)(H_2O)_2Cl_2].Cl_2$	17543(570) 24096(415) 27397(365)	$^1A_1g \rightarrow {}^3T_1g$ $^1A_1g \rightarrow {}^3T_2g$	78.03 (Electrolyte)		Octahedral
$[Pd(L_B)(H_2O)_2].Cl_2$	20746(482) 25773(388) 26109(383)	$^1A_1g \rightarrow {}^1B_1g$ $^1A_1g \rightarrow {}^1E_1g$	72.34 (Electrolyte)	0	Square planer
$[Co(L_B)(H_2O)_2Cl_2]$	34602(289) 26881(372) 21645(462) 14771(677)	IL $^4A_2$ (F) $\rightarrow$ $^4T_1$(P) $^4A_1$ (F) $\rightarrow$ $^4T_1$(F) $^4A_2$ (F) $\rightarrow$ $^4T_2$(F)	16.21 (Non-Electrolyte)	4.73	Octahedral

CT = Charge of Transfer IL = Intra of Ligand.

The curve suggests an increase in the degree of branching in Fig. 11 (α), due to the occurrence of cross-linking. The formation of insoluble material during irradiation further supports the idea that cross-linking is acquiring according to through Eq. (2). Randomly distributed weak bond links, which break down quickly in the early stages of photodegradation, contribute to the degree of deterioration, denoted as α.

m = Primitive of molecular weight.

$$\alpha = mxS/\overline{Mv} \quad (2)$$

The degree of polymerization (DP), monomer unit's number of PVC, the primary phases of PVC is shown in Fig. 12 and Eq. (3), which represents the degree of irradiation. The reverse polymerization (l/DP_n) of the inverted sample compared to the blank sample represents an increase in time of irradiation (l/DP_n).

Mn = the number average molecular weight.

$$Dp_n = X_n = \frac{M_n}{M_o} \quad (3)$$

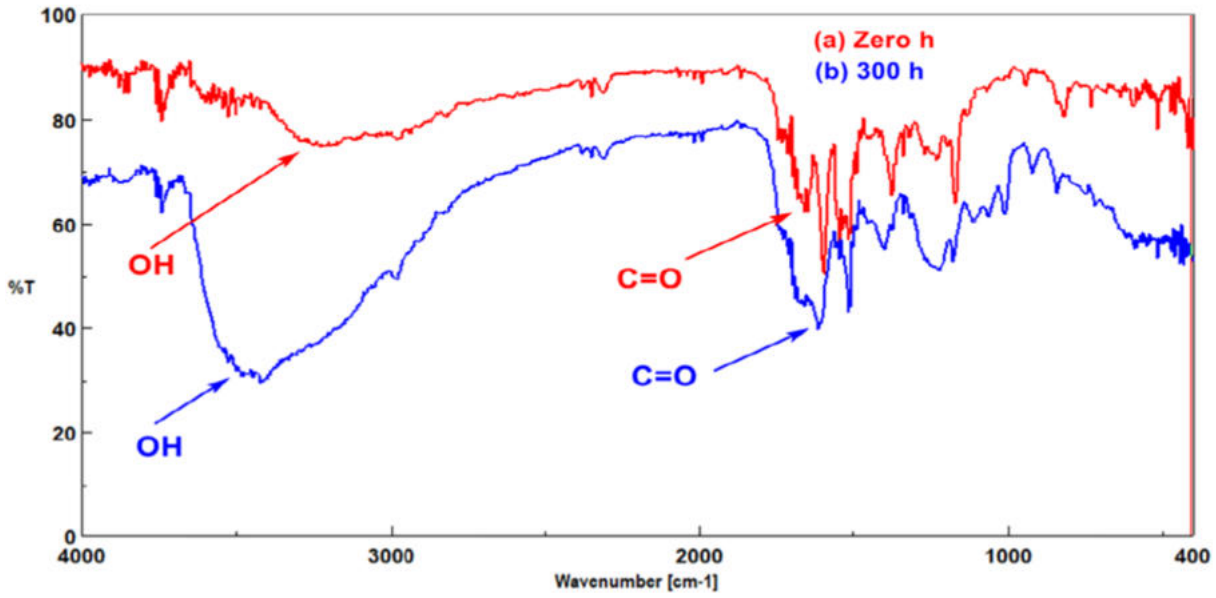

Fig. 4. The Infrared spectra of a polyvinyl chloride film: (a) after and (b) before 300hrs of radiation.

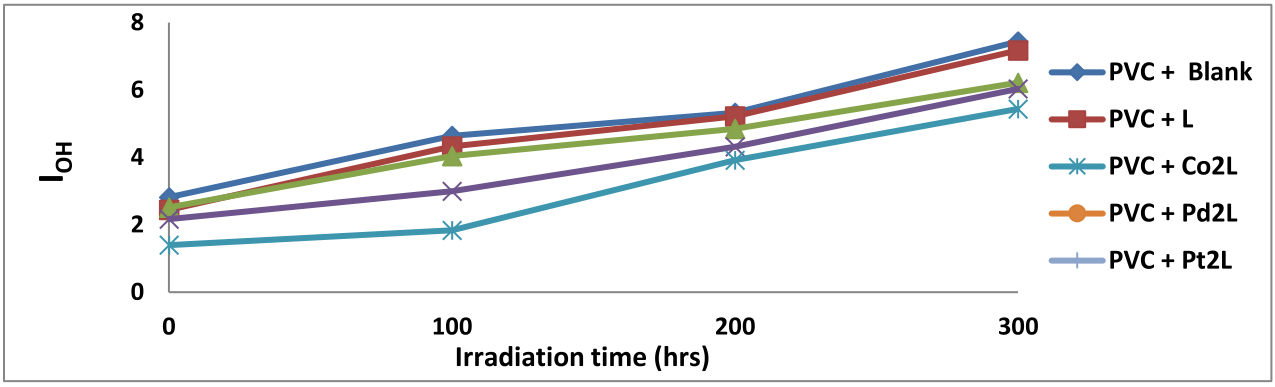

Fig. 5. The relationship between (I_{OH}) and irradiation time of polyvinyl chloride films(40μm) with 0.5% additives.

The UV-light stability for each different polymer films in these additive polymers is determined by the first-order-rate constant (Kd), [23] which is consistently low for photo-stabilizers. Photo-stabilizers, which are additives in PVC films, affect the Kd values. The reduction of Kd values follows the sequence show in Table 6.

The efficiency of the assessed photo-stabilizers [24] was proven to follow the following sequence: PtL_B > PdL_B > CoL_B > L_B > PVC blank

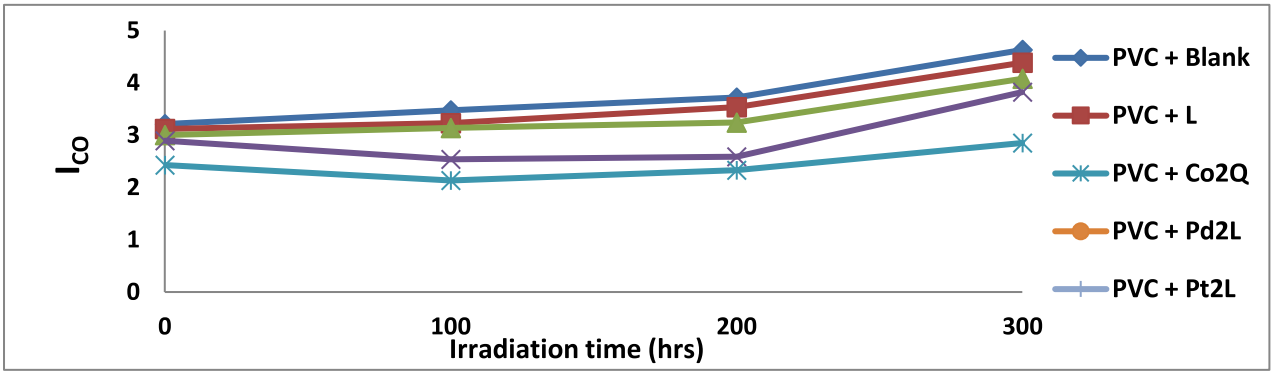

Fig. 6. The relationship between (I_{CO}) and irradiation time of polyvinyl chloride films(40μm) with 0.5%additives.

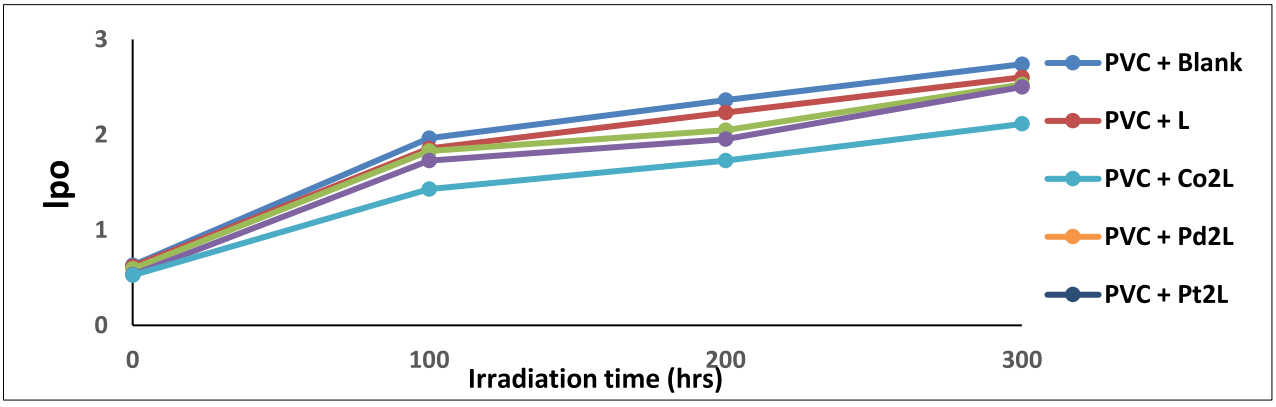

Fig. 7. The relationship between (I_{PO}) and irradiation time of Polyvinyl chloride films(40μm) with 0.5%additives.

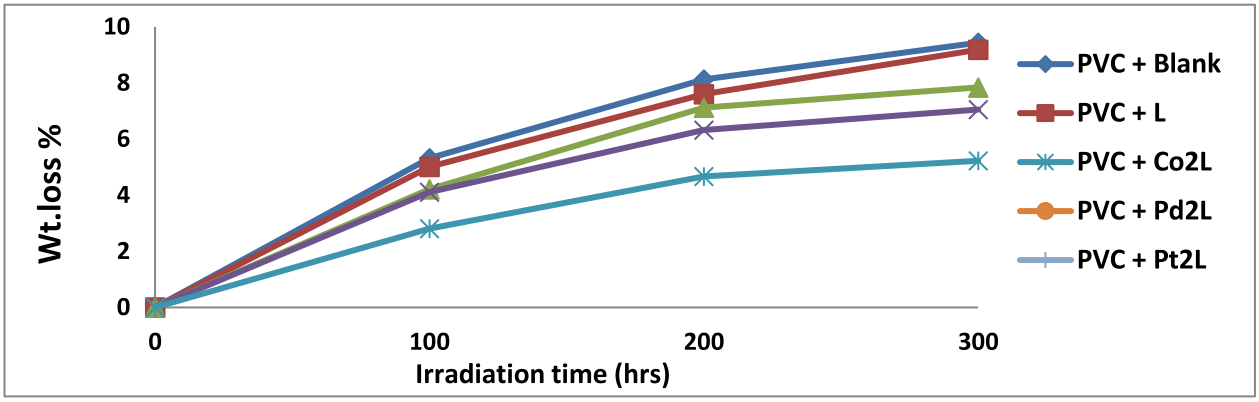

Fig. 8. Relationship between weight loss of (Polyvinyl chloride films (40 μm) + 0.5% additives) with time of irradiation.

Table 6. The Kd of Polyvinyl chloride films thickness (40μm) with 0.5 % additives.

Comp.	K_d (S^{-1})
PVC + Blank	$9.172 * 10^{-3}$
PVC + L_B	$7.529 * 10^{-3}$
PVC + Co_2L_B	$5.918 * 10^{-3}$
PVC + Pd_2L_B	$2.648 * 10^{-3}$
PVC + Pt_2L_B	$2.072 * 10^{-3}$

K_d = Photodecomposition rate constants

Stabilization mechanisms for PVC additives have been proposed

The presence of the thiazole derivative ring is essential of the photo-stabilization of UV-light absorption through peroxide degeneration and radical scavenging. While being absorbed, the UV energy of the aromatic ring decreases,[25] which affects the stability of PVC photography. All this work on film stabilization utilized the resonance resonant suggested in Scheme 2. It is possible that the group of molecules responsible for absorbing light, known as chromophores,[26] may form empty spaces inside their structure owing to the transfer of energy between the molecules and the persistent excitement of the chromophores. The film stabilization work focuses on using resonance to achieve stability. Extended exposure to UV radiation causes the degradation of polymer bonds (C-C). Due to the impacts of photo-stabilization and photo-degradation, this technique may result in very inefficient energy transfer in polymers. Energy exchange occurs between the donor represented by the catalyst polymer molecule and the acceptor represented by the photostable molecules. Energy transfer occurs within molecules between the donor represented by another chromophore[27] and the acceptor represented by the polymer molecules.

Surface morphology for PVC photo degradation evaluation

The sequence of individual polymer chains may be viewed, and in some instances, it is possible to detect single atoms. Despite the widespread usage and popularity of microscopic[28] methods in the study of polymers, there is less knowledge on their use in studying polymer breakdown processes.The most important main reactions in samples irradiated

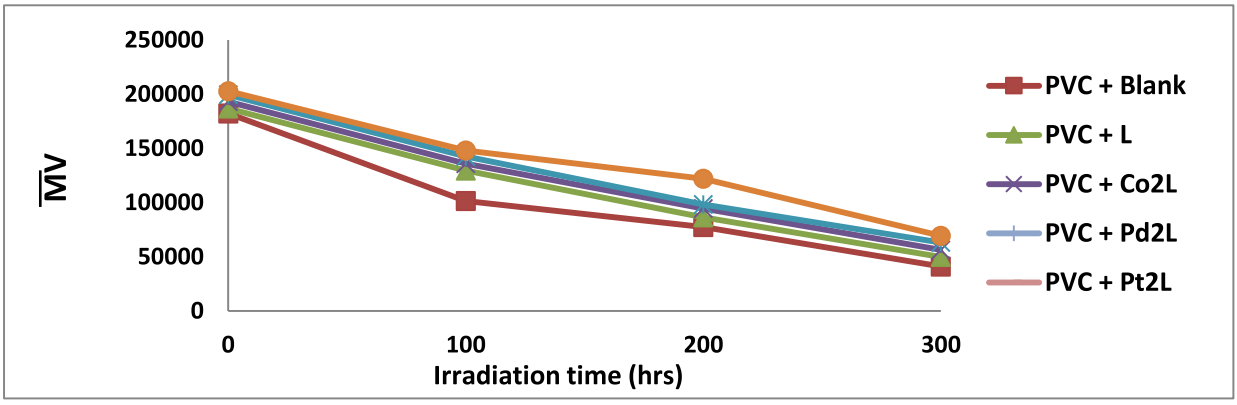

Fig. 9. Relationship between M.wt. average of (Polyvinyl chloride films (40 μm) + 0.5% additives) with time of irradiation.

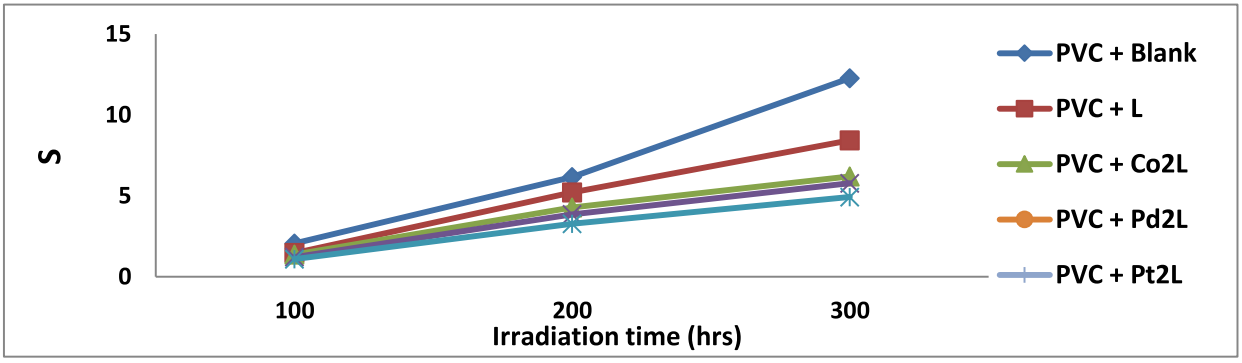

Fig. 10. Relationship between Increase growths in branching degree (S) of (Polyvinyl chloride films (40 μm) + 0.5% additives) with time of irradiation.

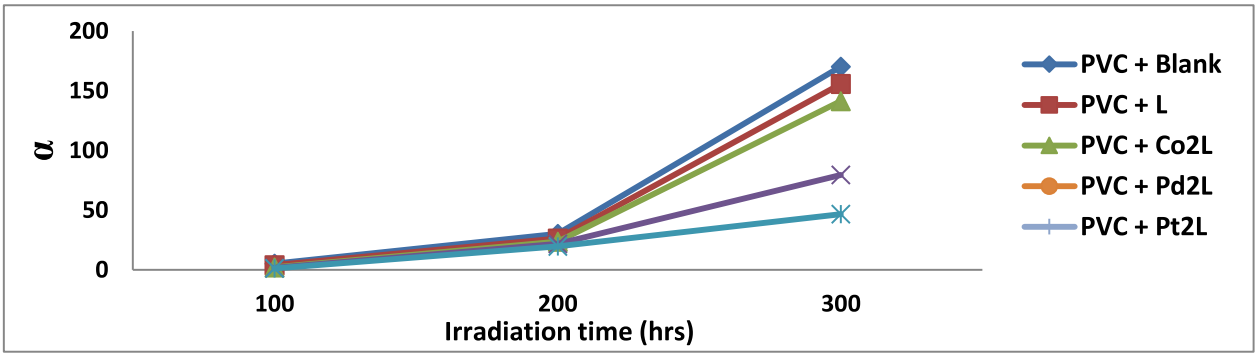

Fig. 11. Relationship between degradation degrees (α) of (Polyvinyl chloride films (40 μm) + 0.5% additives) with time of irradiation.

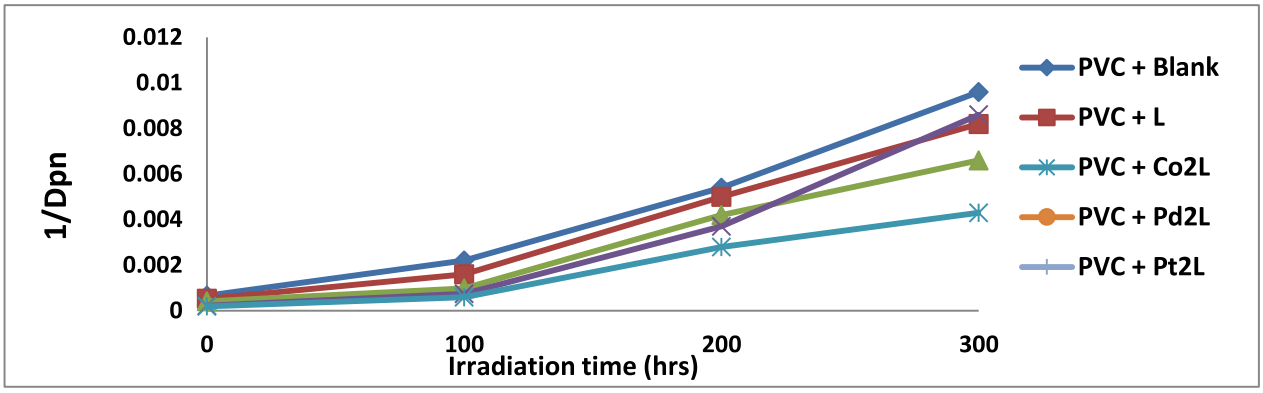

Fig. 12. Relationship between polymerization degrees (1/DPn) of (Polyvinyl chloride films (40 μm) + 0.5% additives) with time of irradiation.

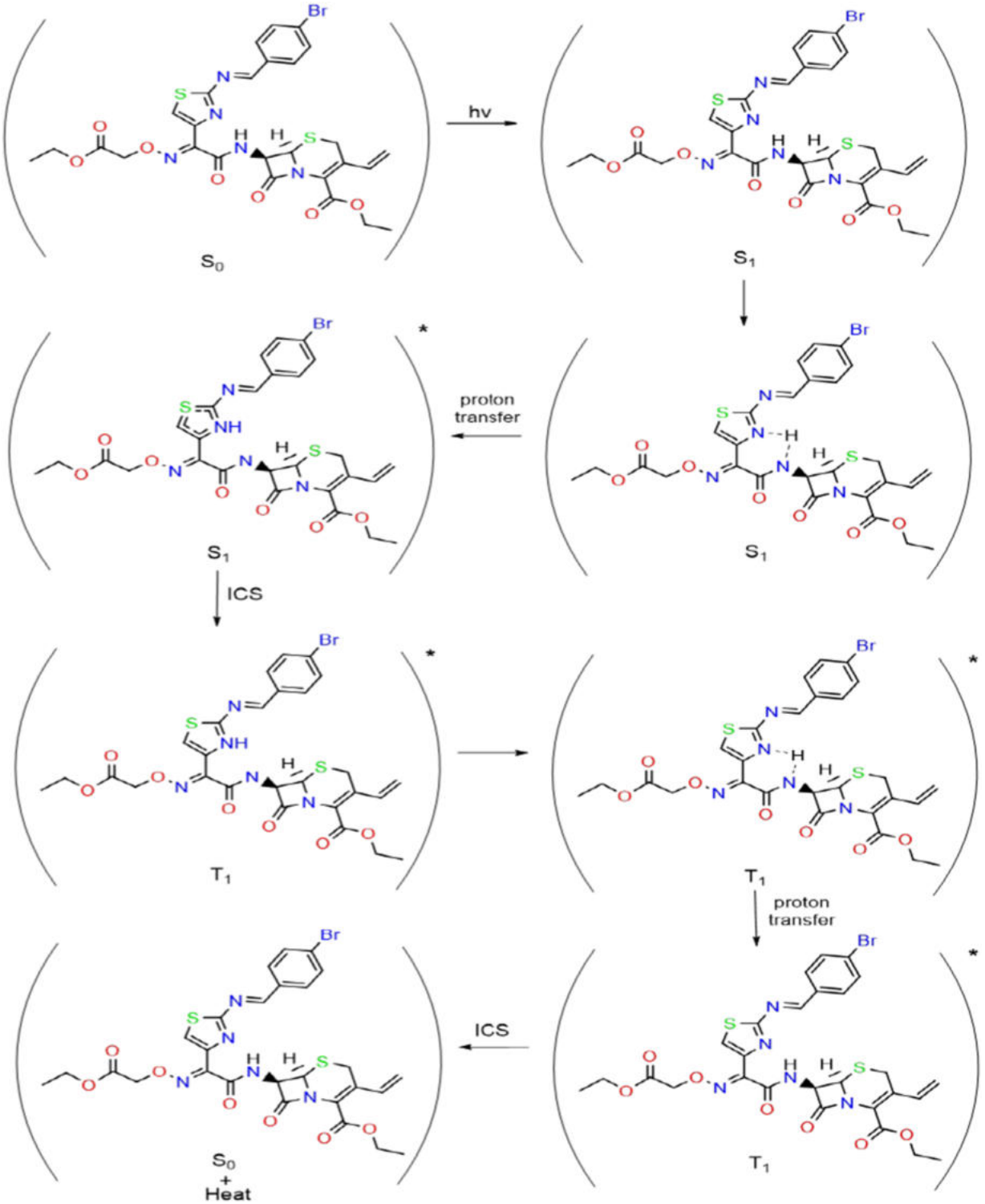

Scheme 2. Proposed mechanism of action for photo-stabilization of Polyvinyl chloride with L^B ligand by dissipation of light energy as heat & absorption of UV light.

with ultraviolet light are branching, cross-linking and division, polyene formation, cross-linking, rearrangement activities, and oxidation of hydroperoxide and hydroxyl groups. Oxidation processes are widely observed on the surface of the sample and are affected by its shape. Photo degradation accelerates subsequent degradation of samples due to the increased free radical-forming activity of the medium and its

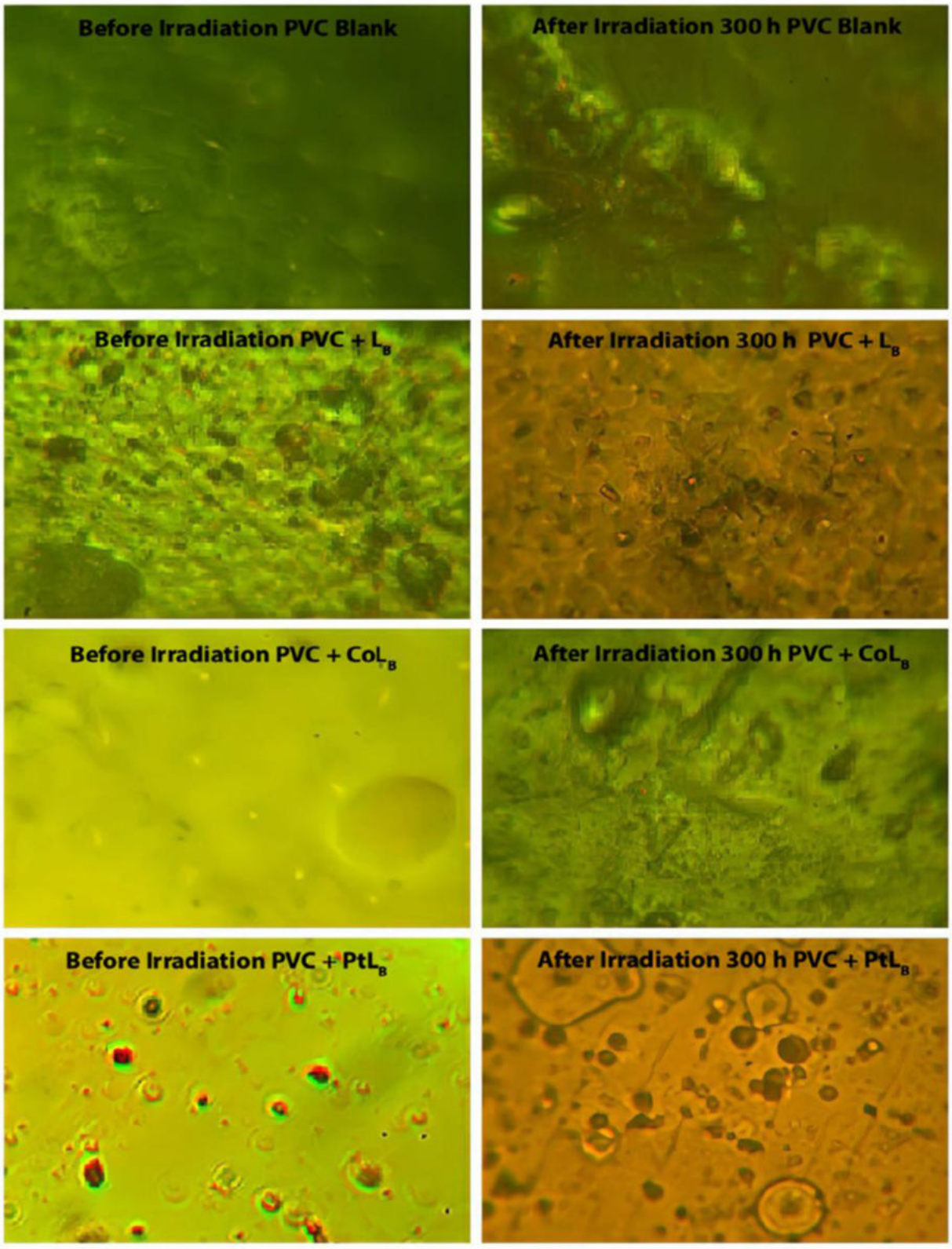

Fig. 13. Images of microscopic for blank Polyvinyl chloride films (40 μm) and the films of their complexes, Morphology of Surface(460× magnification) after and before 300 hrs of irradiation.

sensitivity to light. Exposure also causes samples to become brittle and change color, while films decrease in size. The degradation and transformation of volatile materials leads to the formation of cracks and holes in them. Fig. 13 displays microscopy images of polyvinyl chloride being exposed to (300 hrs.) of U.V-light in this experiment was to initiate polymer decomposition by allowing active free radicals[29] to remove hydrogen atoms from macromolecules.[30] It was observed that crack development in PVC films, without any additives, increased with longer exposure to irradiation. As photo-degradation occurred with U.V-light, the film became more brittle. In contrast, PVC samples treated with Co^{+2} and Pt^{+4} complexes showed lighter cracks, indicating a different level of photodegradation. The occurrence of a chain cleavage-type reaction in photolyzed samples is directly related to the microcracks appearing on the polymer surface. When polymer linkages are disrupted, The resulting fragments represent a larger volume than the original giant particles.[31] The polymer film exposed to UV radiation can experience damage because of the creation of micro - cracks caused by the strains and stresses resulting from the breakdown of internal defects like cracks or impurities. This phenomenon often leads to the formation of cracks. In contrast, PVC film that has not undergone degradation does not possess a distinct micro-structure and appears smooth without any visible structural flaws. Polymers exposed to UV light typically develop small pores of different shapes and sizes when volatile degradation products escape. For instance, a photodegraded PVC film exhibited holes caused by the removal of hydrogen atoms and the breaking of the polymer's main chain. The chemical structure of PVC is composed of ethylene and chloride groups, which results in the formation of gaps and holes. In turn, it increases the diffusion channels for volatile products and the number of adsorbed surfaces, which have a low molecular weight, specifically hydrochloric acid. This causes rapid permeation of oxygen into the polymer package leading to rapid oxidation of the PVC films.

Conclusion

The study focused on synthesizing a bis-dentate Schiff base ligand (L_B) derived from 4-bromobenzaldehyde and forming complexes with three metal ions (Co^{+2}, Pd^{+2}, and Pt^{+4}). The ligand (L_B) binds to M^{+2} or M^{+4} ions via nitrogen and imine groups, in a 1:1 metal-to-ligand molar ratio. The synthesized compounds underwent characterization using various methods including FT-IR, ^{1}H-, ^{13}C-NMR, flame atomic absorption, magnetic measurements, elemental microanalysis, and molar conductivity. These analyses confirmed the proposed geometries of the prepared complexes. The photo-stabilization effectiveness of the compounds was evaluated, revealing the sequence PtL_B > PdL_B > CoL_B > L_B > PVC blank in terms of their ability to stabilize images. The rates of molecular weight decrease, weight loss, and changes in aggregate indicators (hydroxyl, polyene, and carbonyl groups) have been proved. The results demonstrated significant long-term stability, particularly with the platinum complex proving most effective in image stabilization. The study employed rapid photo-degradation assessments of polymeric materials under natural weathering, focusing on UV light-induced degradation of polyvinyl chloride (PVC). Hydroperoxide (POOH) was identified as a key initiator in the photooxidative process. Three metal complexes were synthesized and evaluated as PVC photo-stabilizers at low concentrations against UV radiation. FT-IR spectra indicated minimal absorption bands for PVC containing additives, resulting in less pronounced reductions in PVC weight and mitigated undesired morphological changes. The ligand and its cobalt, palladium, and platinum complexes enhanced the photostability of PVC films by acting as UV radiation absorbers and scavengers for hydrogen chloride and peroxides. The platinum complex, in particular exhibited high effectiveness in inhibiting PVC photodegradation due to its elevated aromatic content, thereby posing no environmental concerns after use.

Acknowledgment

Sincere thanks and appreciation to the staff of the Chemistry Department for their cooperation throughout the research period.

Authors' declaration

- Conflicts of Interest: None.
- We hereby attest that all of the manuscript's figures and tables are ours. Additionally, permission has been provided for the re-publication of figures and images, which are not ours and are connected to the manuscript.
- No animal studies are presented in the manuscript.
- No human studies are presented in the manuscript.
- Ethical Clearance: The project was approved by the local ethical committee at University of Baghdad.

Authors' contribution statement

The authors I.Kh.J. and E.J.W. participated in preparing ligand and the metal complexes and identifying them. By performing various spectral measurements to identify the newly prepared compounds and collecting, analyzing and interpreting the data, inserting shapes, diagrams and chemical structures for this purpose. The author A.M.A. performed the photostability studies on the prepared compounds, conducting all analyses related to these studies, collecting and interpreting their data, and including their graphs. In addition, all authors participated in writing the manuscript, rephrasing the statements appropriately, formatting them within the journal template, and including the references for each paragraph. All authors carefully read the manuscript and approved the final version sent to your esteemed journal.

References

1. Pillai MS, Latha SP. Designing of some novel metallo antibiotics tuning biochemical behaviour towards therapeutics: Synthesis, characterisation and pharmacological studies of metal complexes of cefixime. J Saudi Chem Soc. 2016;20:60–66 https://doi.org/10.1016/j.jscs.2012.09.004.
2. Khurana P, Pulicharla R, Brar SK. Antibiotic-metal complexes in wastewaters: Fate and treatment trajectory. Environ Int. 2021;157:1–9 https://doi.org/10.1016/j.envint.2021.106863.
3. Ali AJ, Abbas MT, Hamdan IAA, Hamdan AA. Novel synthesis, characterization, antibacterial evolution & molecular modeling of Schiff base derived from R-camphor & five antibiotics from third generation of cephalosporin. In IOP Conf Ser Mater Sci Eng; 2019: IOP Publishing.p. 1–18 https://dx.doi.org/10.1088/1757-899X/571/1/012091.
4. Awf AR, Waheed EJ, Ahmed TN. Synthesis, characterization and anticorrosion studies of new Co(II), Ni(II), Cu(II), and Zn(II) schiff base complexes. Int J Drug Deliv Technol. 2021;11(2):414–422 https://doi.org/10.1088/1742-6596/1660/1/012109.
5. Yoshikawa N, Shibasaki M. Catalytic asymmetric synthesis of β-hydroxy-α-amino acid esters by direct aldol reaction of glycinate Schiff bases. Tetrahedron. 2002;58(41):8289–8298 https://doi.org/10.1016/S0040-4020(02)00979-1.
6. Mahmood TS, Numan AT, Waheed EJ. Synthesis, spectroscopic identification and antimicrobial activity of mixed ligand complexes of new ligand [3-((4-acetyl phenyl) amino)-5, 5-dimethylcyclohex-2-en-1-one](hl*) with 3-amino pheno. Biochem Cell Arch. 2020;20(1):2235–2245 https://doi.org/10.35124/bca.2020.20.1.2235
7. Boczar D, Michalska K. Cyclodextrin inclusion complexes with antibiotics and antibacterial agents as drug-delivery systems—A pharmaceutical perspective. Pharmaceutics. 2022;14(7):1–71 https://doi.org/10.3390/pharmaceutics14071389.
8. Habeeb MR, Morshedy SM, Daabees HG, Elonsy SM. Development, validation and greenness assessment of a new electro-driven separation method for simultaneous analysis of cefixime trihydrate and linezolid in their fixed dose combination. BMC Chem. 2023;17(1):132–148 https://doi.org/10.1186/s13065-023-01049-3.
9. Makinta As, Mohammed Bf, Ndahi Np, Ahmed Aa, Mahmud Mm. Mechano and solvent-based syntheses, characterization and antimicrobial activity of cefexime and cefuroxime with their Pb (II) complexes. JASAB. 2022;4(1):2043–2049 https://doi.org/10.48402/IMIST.PRSM/jasab-v4i1.31543.
10. Al-Thubaiti EH, El-Megharbel SM, Albogami B, Hamza RZ. Synthesis, spectroscopic, chemical characterizations, anticancer capacities against HepG-2, antibacterial and antioxidant activities of cefotaxime metal complexes with Ca (II), Cr (III), Zn (II), Cu (II) and Se (IV). Antibiotics. 2022;11(7):967–991 https://doi.org/10.3390/antibiotics11070967.
11. Thakur J, Mohan S. Comparison of antimicrobial activity of triple, double, and cefixime-based antibiotic pastes against enterococcus faecalis: An in vitro study. Cureus. 2023;15(8):1–5 https://doi.org/10.7759/cureus.44024.
12. El-Megharbel SM, Qahl SH, Alaryani FS, Hamza RZ. Synthesis, spectroscopic studies for five new Mg (II), Fe (III), Cu (II), Zn (II) and Se (IV) ceftriaxone antibiotic drug complexes and their possible hepatoprotective and antioxidant capacities. Antibiotics. 2022;11(5):547–568 https://doi.org/10.3390/antibiotics11050547.
13. Tumpa JB, Islam MS. Antibiotic with essential metals complexation and interaction: An In vitro study by spectrophotometric method. Am J Biomed Res. 2019;3(1):90–93 https://doi.org/10.34297/AJBSR.2019.03.000640.
14. Berber N. Preparation and characterization of some Schiff base compounds. Adv J Sci. 2020;10(1):179–188 https://doi.org/10.37094/adyujsci.633080.
15. Balachandran G, Dhamotharan A, Kaliyamoorthy K, Rajammal KS, Kulandaiya R, Raja A. Synthesis, characterization, and catalytic applications of schiff-base metal complexes. Eng Proc. 2024;61(1):26–33 https://doi.org/10.3390/engproc2024061026.
16. Al-Khazraji AMA. Synthesis of Co (ll), Ni (ll), Cu (ll), Pd (ll), and Pt (lV) Complexes with 14, 15, 34, 35-Tetrahydro-11 H, 31 H-4, 8-diaza-1,3 (3,4)-ditriazola-2,6 (1,4)-dibenzenacyclooctaphane-4,7-dien-15, 35-dithione, and the thermal stability of polyvinyl chloride modified complexes. Indones J Chem. 2023;23(3):754–769 https://doi.org/10.22146/ijc.81272.
17. Safikhani-Golboos R, Ghorbanloo M, Bikas R, Sasani R, Małecki JG, Krawczyk MS, *et al.* Manganese (II) coordination compounds of thiazole-hydrazone based NNN-donor ligands: Synthesis, characterization and catalytic activity. Inorganica Chimica Acta. 2022;543:121–148 https://doi.org/10.1016/j.ica.2022.121188.
18. Al-Khazraji AM, Al Hassani RA. Synthesis, characterization and spectroscopic study of new metal complexes form heterocyclic compounds for photostability study. Sys Rev Pharm. 2020;11(5):535–555 https://doi.org/10.31838/srp.2020.5.71.
19. Etaiw SEH, Abd El-Aziz DM, Abd El-Zaher EH, Ali EA. Synthesis, spectral, antimicrobial and antitumor assessment of Schiff base derived from 2-aminobenzothiazole and its transition metal complexes. Spectrochimica Acta Part A: Molecular Biomolecular Spectroscopy. 2011;79(5):1331–1337 https://doi.org/10.1016/j.saa.2011.04.064.
20. Kumar K, Mishra N, Anand SR, Shrivastava SP. Synthesis and properties of transition metal complexes containing thiazole derived schiff base ligands. Orient J Chem. 2022;38(5):1209–1216 https://doi.org/10.13005/ojc/380516.
21. Abd AL_Qadir NA, Shaalan ND. Synthesis, characterization and biological activity study for some new metals complexes with (3Z, 3'E)-3, 3'-(((2E, 5E)-hexane-2, 5-diylidene)

bis (hydrazine-2, 1-diylidene)) bis (indolin-2-one). IBN A-Haitham J Pure Appl. Sci. 2023;36(3):231–244 https://doi.org/doi.org/10.30526/36.3.3071.
22. Hashim DJ, Waheed EJ, Hadi AG, Baqir SJ. Exploring the biological activity of organotin carboxylate complexes with 4-sulfosalicylic acid. Bull Chem Soc Ethiop. 2023;37(6):1435–1442 https://doi.org/10.4314/bcse.v37i6.11.
23. Seo HJ, Lee JW, Na YH, Boo J-H. Enhancement of photocatalytic activities with nanosized polystyrene spheres patterned titanium dioxide films for water purification. Catalysts. 2020;10(8):886–898 https://doi.org/10.3390/catal10080886.
24. Watheq B, Yousif E, Al-Mashhadani MH, Mohammed A, Ahmed DS, Kadhom M, *et al.* A surface morphological study, poly (vinyl chloride) photo-stabilizers utilizing ibuprofen tin complexes against ultraviolet radiation. Surf Interfaces. 2020;3(4):579–593 https://doi.org/10.3390/surfaces3040039.
25. Ankamah E, Sebag J, Ng E, Nolan JM. Vitreous antioxidants, degeneration, and vitreo-retinopathy: exploring the links. Antioxidants. 2019;9(1):7–27 https://doi.org/10.3390/antiox9010007.
26. Chamas A, Moon H, Zheng J, Qiu Y, Tabassum T, Jang JH, *et al.* Degradation rates of plastics in the environment. ACS Sustain Chem Eng. 2020;8(9):3494–3511 https://doi.org/10.1021/acssuschemeng.9b06635.
27. Yousif E, Ahmed DS, Ahmed AA, Hameed AS, Muhamed SH, Yusop RM, *et al.* The effect of high UV radiation exposure environment on the novel PVC polymers. Environ Sci Pollut Res Int. 2019;26:9945–9954 https://doi.org/10.1007/s11356-019-04323-x.
28. Hendrickson E, Minor EC, Schreiner K. Microplastic abundance and composition in western Lake Superior as determined via microscopy, Pyr-GC/MS, and FTIR. Environ Sci Technol. 2018;522(4):1787–1796 https://doi.org/10.1021/acs.est.7b05829.
29. Gao Y, Zhou D, Lyu J, Xu Q, Newland B, Matyjaszewski K, *et al.* Complex polymer architectures through free-radical polymerization of multivinyl monomers. Nat Rev Chem. 2020;4(4):194–212 https://doi.org/10.1038/s41570-020-0170-7.
30. Kharlampenkov E, Kudryashova I, Zakharova N, Loginova A. Environmental aspects of technology and technical support of PVC production based on clustering of the economy. In E3S Web Conf; 2021;1–8. https://doi.org/10.1051/e3sconf/202127802013.
31. AL-Khazraji SIC, Sadik WM, Ahamed LS. Synthesis and characterization of New 2-amino-5-chlorobenzothiazole derivatives containing different types of heterocyclic as antifungal activity. Baghdad Sci J. 2024;21(3):0962–0974 https://doi.org/10.21123/bsj.2023.8318.

تحضير وتشخيص طيفي ودراسات الاستقرار الضوئي لليكاند جديد مشتق من 4-بروموبنزالدهيد ومعقداته الفلزية

ايناس جاسم وحيد، علي مضر عبد الكريم الخزرجي، ابتسام خليفة جاسم

قسم الكيمياء، كلية التربية للعلوم الصرفة – ابن الهيثم، جامعة بغداد، بغداد، العراق.

الخلاصة

تم تحضير ليكاند قاعدة شف جديد (L_B) من التفاعل الكيميائي للمادة الوسطية (P) و4-بروموبنزالدهيد. ثلاثة معقدات جديدة ذات الصيغة العامة $[Pd(L_B)(H_2O)_2].Cl_2$ (مربع مستوي) و $[M(L_B)(H_2O)_2Cl_2].mCl_2$ (ثماني السطوح)، حيث m=0 في Co^{+2} و 1 في Pt^{+4} ناتجة من تفاعل ليكاند قاعدة شف الجديد (L_B) [إيثيل (6ر,7ر) -7- ((اي)-2-(((((اي)-4-بروموبنزلديهايد)امينو)ثايازول-4-يل)-2-((2-يثوكسي-2-وكسويثوكسي)امينو)استمايدو)-8-وكسو-3-فنيل-5-ثايا-1-ازابايسكلو[0.2.4] وكت-2-ين-2-كاربوكسيليت](L_B) مع الأيونات الفلزية المذكورة. تم تشخيص الليكاند (L_B) ومعقداته الفلزية بواسطة بعض التقنيات ومنها طيف الرنين النووي المغناطيسي البروتوني والكاربوني وطيف الاشعة تحت الحمراء وطيف الاشعة فوق البنفسجية-المرئية والقياسات المغناطيسية والتحليل الدقيق للعناصر والتوصيلية المولارية. الاستقرار الضوئي للبوليمرات يهتم بإزالة أو تأخير العملية الكيميائية الضوئية في المواد البلاستيكية والبوليمرات التي تحدث أثناء عملية التشعيع. في (THF) رباعي هيدرو الفوران، تم خلط المركبات المحضرة (الليكاند L_B ومعقداته الفلزية) مع وزن/وزن 0.5% من (PVC). تحت إشعاع الضوء nm (380–250) λ بكثافة (25°C) (7.75×10^{-9}) ein dm^{-3} s^{-1}، تمت دراسة الاستقرار الضوئي لأفلام البوليمر. من خلال مراقبة مؤشرات الكربونيل، البوليين والهيدروكسيل، وطريقة زمن التشعيع مع فقدان الوزن، تم تحديد نشاط الاستقرار الضوئي للمركبات المحضرة. حيث لوحظ مع زمن التشعيع، تزداد قيم مؤشر I_{CO} وI_{OH} وI_{PO}، وتعتمد هذه الزيادة على نوع المادة المضافة. كما تمت دراسة زمن التشعيع والشكل السطحي للأفلام. ويعتبر هذا التطبيق مهماً للنظام البيئي من حيث علاقته بتقليل استهلاك البلاستيك.

الكلمات المفتاحية: 4-بروموبنزالدهيد، الاستقرار الضوئي، التحلل الضوئي، المعقدات الفلزية، بولي فينيل كلورايد.